Short Communication

Preparation of ZnO Nanosheets-Nanorods Hierarchically Structured Films and Application in Quantum Dots Sensitized Solar Cells

Zeng Chen, Shengjun Li, Chaochao Wei, Chunli Diao, Qingqing Pei, Junhao Cai, Weifeng Zhang*

Henan Key Laboratory of Photovoltaic Materials, Henan University, Kaifeng 475001, China
*E-mail: lishengjun1011@126.com

ZnO nanosheets were electrodeposited on transparent conductive glass substrates. Thereafter, ZnO nanorods were grown vertically on the nanosheets by hydrothermal method to prepare the nanosheets-nanorods hierarchically structured ZnO films. The influence factors, such as the concentration of precursor solution and the hydrothermal reaction time, were studied. The obtained nanosheets-nanorods hierarchically structured ZnO films were co-sensitized with CdS and CdSe quantum dots and applied as the photoanodes of dye-sensitized solar cells. A photoelectric conversion efficiency of 2.50% was obtained after the coating of TiO_2 on the ZnO nanosheets-nanorods.

1. INTRODUCTION

Dye-sensitized solar cells (DSSCs) have been widely investigated recently due to its low cost and high conversion efficiency. n-DSSC, the most common used DSSCs, though has obtained high conversion efficiency [1], There are still many unexplored factors which could bring further improvement for the DSSCs. One approach is to develop new sensitizers. Specifically, narrow-band-gap semiconductors quantum dots (QDs), such as CdS, CdSe, CdTe and PbS, have attracted much attention because of their tunable band gap, large extinction coefficient, high stability and generation of multiple excitations with single-photon absorption [2-8].

Another strategy is to select new material and design novel structure for electron travelling. Much n-type semiconductors such as TiO_2, SnO_2 and ZnO have been investigated for many years [9-11]. Compared to TiO_2, ZnO have the similar band gap and physical properties, but much higher

electron mobility ($155 cm^2V^{-1}s^{-1}$ vs. $10-5 cm^2V^{-1}s^{-1}$), which enables ZnO to be a good alternative materials to TiO_2[12]. In addition, the structure and morphology of ZnO could be controlled easily [13-15]. These regular structures, such as nanorod, nanotube and nanosheet, provide a direct pathway for the transportation of the photoinduced electron when they were used as photoanodes, which might suppress the charge recombination [16-20]. Nevertheless the insufficient internal surface area of these nanostructures limited the further improvement of the solar conversion efficiency. To increase the internal surface area, 3D-nanostructured ZnO was induced, which could both afford a direct conduction pathway and load more dyes. Tian et al. synthesized a kind of hierarchically structured ZnO nanorods-nanosheets and obtained a high photoelectric conversion efficiency of 3.28% which was about twice as much as that of ZnO nanorod photoelectrode[21]. Xu et al. developed a ZnO nanowire-nanosheet architecture, and sensitized it with N719, resulting in a photovoltaic performance of 4.8%[22]. kuang et al. sensitized 3D hyperbranched TiO_2/ZnO arrays with CdS/CdSe QDs to prepare photoanode and obtained a power conversion efficiency of 4.25% [23]. A. Roy et al. used ZnO nanoparticle as blocking layer and ZnO nanorods as the scattering layer for QDSCs photoanode [24]. L.B. Li et al. prepared hierarchical nanorods-nanosheet structured ZnO film using two-step hydrothermal method. A maximum power conversion efficiency of 4.26% was obtained after the optimization of nanorods growth time [25].

In this paper, we electrodeposited ZnO nanosheets (ZNS) on transparent conductive glass substrates. Then, ZnO nanorods (ZNR) were grown vertically on the nanosheets by hydrothermal method to prepare the nanosheet-nanorod (ZNS-ZNR) structured ZnO films. The influence factors, such as the concentration of precursor solution and the hydrothermal reaction time, were studied. Sequentially, a TiO_2 layer was deposited on the ZNS-ZNR arrays film to prepare ZNS-ZNR/TiO_2 composite film. The obtained composite films were sensitized with CdS/CdSe QDs and the photoelectric properties were investigated.

2. EXPERIMENTAL

2.1 Electrodeposition of vertically aligned ZnO nanosheet arrays

The ZNS were prepared by facile electrodeposition process according to our reported literature earlier. Briefly, the precursor solution consisted of 0.1 M KCl and 0.05 M $Zn(NO_3)_2 \cdot 6H_2O$. The FTO glass substrate (1cm×1cm) was used as working electrode. A Pt foil and an Ag/AgCl electrode were used as counter electrode and reference electrode, respectively. The electrodeposition experiment was carried out with a constant potential of -1.1 V at 70 ℃ for 30 min. Then the samples were rinsed with distilled water, dried at room temperature and annealed at 450 ℃ for 30min in air.

2.2 Synthesis of ZNS-ZNR arrays and TiO_2 coating

The ZNS-ZNR arrays were fabricated by a facile hydrothermal process. In detail, an equi-molar concentration of $Zn(NO_3)_2 \cdot 6H_2O$ and $C_6H_{12}N_4$ (HTMT) were added to 80 ml aqueous solution and stirred for 30 min. The concentration was changed from 0.01 M to 0.05 M. And then the mixed

aqueous solution was transferred to a 100ml Teflon-lined stainless steel autoclave, and the as-prepared ZNS arrays were vertically immersed in the solution. The autoclave was maintained at 90 ℃ in an oven for 10 h. Thereafter, the autoclave was cooled down to the room temperature naturally, and the sample was washed with deionized water and dried at room temperature. Sequentially, the sample was annealed at 450 ℃ in air for 30 min. The as-synthesized ZNS-ZNR arrays were immersed in an aqueous solution of 0.1 M $(NH_4)_2TiF_6$ and 0.2 M H_3BO_3 for a coating of TiO_2 layer. The ZNS-ZNR/TiO_2 hybrid films were calcined at 450 ℃ for 60 min in air.

2.3 CdS/CdSe co-sensitized photoanodes and DSSCs fabrication

The SILAR method was used for the deposition of CdS QDs. The as-prepared samples ZNS-ZNR/TiO_2 were first dipped into an ethanol solution containing 0.2 M $Cd(NO_3)_2$ for 1 min, rinsed with ethanol, and then dipped into 0.2M Na_2S methanol solution for another 1 min and rinsed again with methanol. This two-step dipping procedure was repeated for 7 times. For the deposition of CdSe, The CdS QDs sensitized ZNS-ZNR/TiO_2 films were immersed in a mixed aqueous solution (Na_2SeSO_3, 80 mM Cadmium Sulfate and 120 mM trisodium nitrilotriacetate monohydrate with a volume ratio of 1:1:1) for 7 h at room temperature and then rinsed with deionized water.

For DSSCs fabrication, the as-prepared samples were used as photoanodes and assembled with a Cu_2S counter electrode in a sandwich type, and then the polysulide electrolyte was injected into the space. The Cu_2S counter electrode was prepared as follows, an aqueous solution (40 ml) of 1 M copper(II) sulfate pentahydrate was slowly added to 40 ml aqueous solution of thiourea (50 mM) at room temperature. Then the solution was quickly transferred to autoclave, filling 80% volume. FTO substrate was leaned against the wall of the Teflon-liner with the conducting side facing down. Subsequently, the autoclave was moved into the oven and maintained for 8 h at 100 ℃. Polysulfide electrolyte was an aqueous solution containing 1 M Na_2S, 1 M S and 0.1 M NaOH.

2.4 Measurement and characterization

The morphology and structure of ZNS-ZNR arrays were studied by a JSM-7001F field emission scanning electron microscope SEM). The crystalline phase of the samples was characterized using a DX-2700 X-ray diffraction meter (XRD) with a monochromatized Cu K_a irradiation (λ= 0.154145 nm). The absorption spectra were obtained from UV−VIS photospectrometer (Varian Cary 5000).

The photovoltaic performance of DSSCs was measured using a Keithley 2440 sourcemeter under AM 1.5G illumination from a Newport Oriel Solar Simulator with an intensity of one sun. The incident light intensity was calibrated with a standard Si solar cell provided by Newport Oriel. The active cell area of the assembled QDs sensitized solar cells (QDSCs) was 0.25 cm^2. The incident photon-to-current conversion efficiency (IPCE) spectra were measured by an IPCE system designed especially for QDSCs (Crowntech. Inc.). A 150W tungsten halogen lamp was used as the light source to generate a monochromatic beam. A silicon solar cell was used as the standard during calibration.

IPCE values were measured using a Keithley model 2400 source meter. The dark currency was measured on an electrochemistry workstation (CHI660b).

3. RESULTS AND DISCUSSION
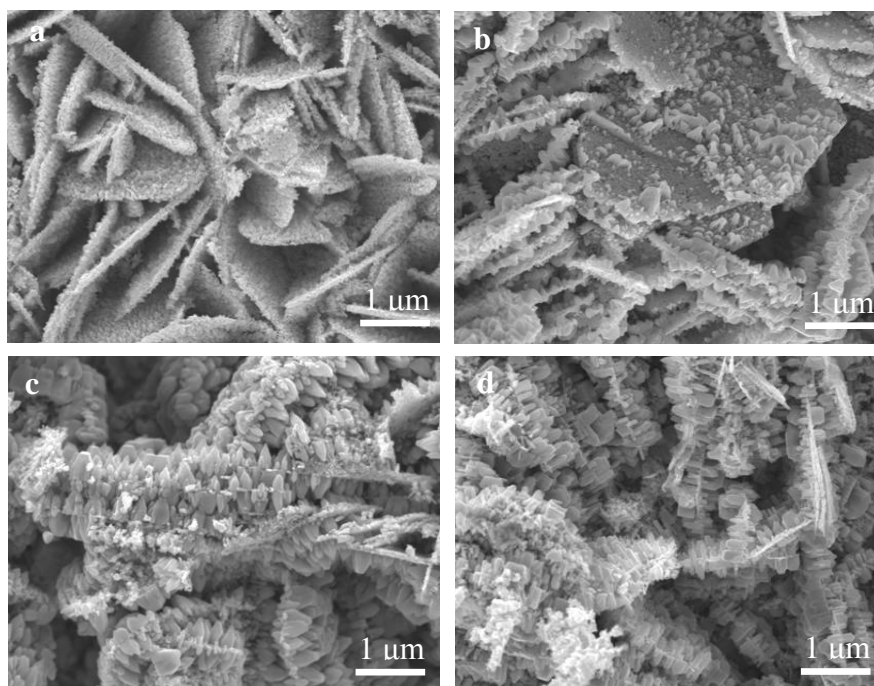
Figure 1. SEM images for the samples of ZNS before hydrothermal treatment (a) and after hydrothermal treatment with different HTMT concentration, 0.01M (b), 0.03M(c) and 0.05M (d).
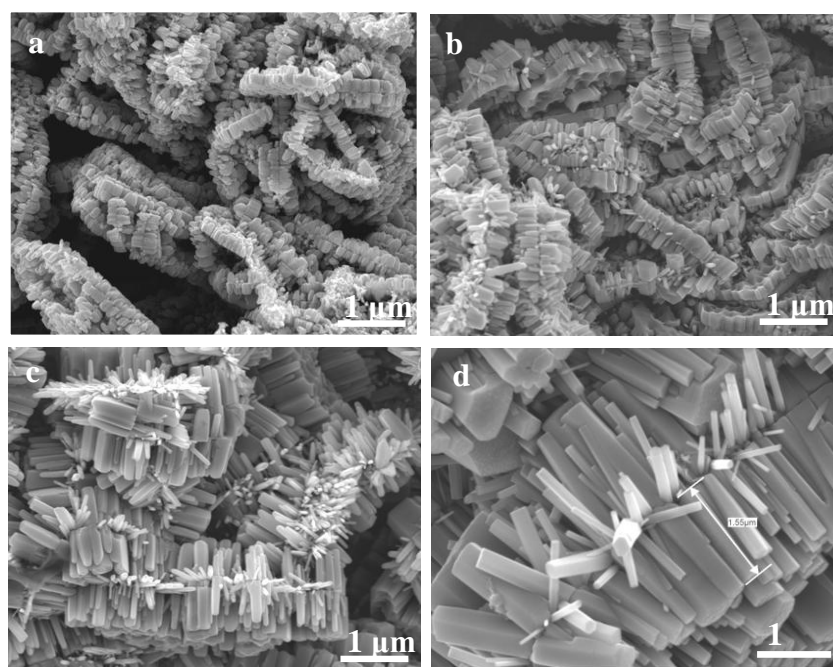

Figure 2. SEM images for the samples of ZNS prepared with different hydrothermal reaction time: (a) 4 h; (b) 8 h; (c) 10 h; (d) 12 h

The micrographs for the morphology of as-prepared ZNS-ZNR ZnO arrays were displayed in Figure1. Among them, Figure 1 (a) shows the ZNS arrays prepared by electrodepostion method. It can be seen that the ZnO nanosheets are almost vertical to the substrates. Figure 1 (b-d) show the micrographs of ZNR arrays after hydrothermal treatment with different concentration of $Zn(NO_3)_2$ and HTMT. The precursor solution concentration was controlled to be 0.01M, 0.03M and 0.05M, respectively. The treatment time was all controlled to be 6 h.

The morphology of ZnO samples obviously changed with the increasing of precursor solution concentration. When the precursor solution concentration was 0.01 M, only a few tiny protrusions grow on nanosheets (Figure 1 (b)) which should be contributed to the lack of zinc ion. When the precursor solution concentration increased from 0.01 M to 0.03 M (Figure 1 (c)), both sides of the nanosheets were covered with cones. When the precursor solution concentration was 0.05 M (Figure 1(d)), regular ZnO nanorods with high density was observed. However, the length of the ZnO nanorods grown on the nanosheets was much short which could not fulfil the requirements of large specific area for photoanode.

In order to obtain longer nanorods, the hydrothermal treatment time was also optimized. The SEM images of ZnO NS-NR arrays with different growth time were presented in Figure 2 (a-d). The growth time was 4 h, 8 h, 10 h and 12h. It can be seen that a large number of protrusions cover on both sides of the nanoplates, which was the prototype of the nanorods when the reaction time was 4 h (Figure 1(a)). With the extension of the reaction time, the nanorods grew longer and longer (shown in Figure 2 (a-d)). When the time was 10 h, the length of the nanorod was ca. 1.5 μm which was much attractive for the photoanode [21].
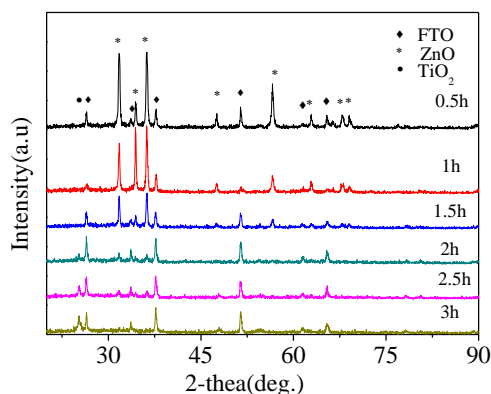

Figure 3. XRD of the ZNS-ZNR before and after treatment of $(NH_4)_2TiF_6$ aqueous solution for different time

The obtained ZnO NS-NR arrays were applied to prepare photoanode for QDSCs. It is known that coating ZnO with a TiO_2 layer could suppress the charge recombination of ZnO photo anode and improve the open circuit voltage of DSSCs. The ZnO ZNS-ZNRs arrays was coated withTiO_2 using $(NH_4)_2TiF_6$. Figure 3 gives the X-ray diffraction (XRD) patterns for the samples obtained by treating the ZnO ZNS-ZNR arrays with $(NH_4)_2TiF_6$ aqueous solution for different time. Before the $(NH_4)_2TiF_6$

treatment, all the diffraction peaks were indexed to be the hexagonal ZnO in accordance with the standard card PCDS 36-1451 except that of FTO glass substrate. With the increasing of immersion time, it is easily observed that the intensity of ZnO diffraction peaks decreased quickly. The diffraction peak of TiO_2 appeared when the immersion time was 2 h. The Intensity of this peak continued to increase with the immersion time extension. The diffraction peaks of ZnO disappeared when the immersion time was 3 h which indicated that ZnO might be converted to TiO_2 completely. The treatment time was controlled to be 1 h in the following experiments.

The QDSCs were assembled using CdS/CdSe QDs sensitized ZNS, ZNS/TiO_2 and ZNS-ZNR/TiO_2 films as photoanodes. The photocurrent-voltage curves were measured under 1 sun illumination and shown in Figure 4 (a). Their photovoltaic characteristic parameters wee listed in Table 1. The QDSCs based on ZNS films presented a power conversion efficiency of 1.31%. After $(NH_4)_2TiF_6$ treatment, the short circuit current density (J_{sc}) showed almost no change. But the open circuit voltage (V_{oc}) increased from 0.485V to 0.599V. Furthermore, the fill factor (*ff*) was also improved. As a result, the efficiency of QDSCs increased to 1.85%, which should be attributed to the suppression of charge recombination at the interfaces between ZNS and QDs, or electrolyte. The similar results had been found by Chen et al. that suitable TiO_2 coating on ZnO nanosheets through $(NH_4)_2TiF_6$ treatment significantly increased the photo-excited electron lifetimes and consequently improved the open-circuit voltage and fill factor of the QDSCs [20]. The QDSCs based on ZNS-ZNR/TiO_2 photoanodes showed a high J_{sc} of 8.51 mA/cm^2, which was much higher than that assembled with ZNS or ZNS/TiO_2 photoanode. The power conversion efficiency was enhanced to be 2.50%. It should be attributed to the enlargement of the specific area after the grown of ZnO nanorods on the nanosheets which could load more QDs. J.J. Tian et al. confirmed this conclusion through nitrogen sorption isotherms, which indicated that the hierarchical nanorods-nanosheets structured ZnO film showed about twice specific surface area of that of ZnO nanorods film [21]. Another reason for this result might be the enhancement of the electron transport property of ZNS-ZNR/TiO_2 photoelectrodes [25]. The dark current-voltage properties of QDSCs based on different ZnO photoanodes was also measured to investigate recombination reaction. The dark current-voltage curves were shown in Figure 4(b). It can be observed that the dark current was significantly suppressed after the coating of TiO_2. There was no obvious difference between the ZNS/TiO_2 and ZNS-ZNR/TiO_2 photoelectrodes which indicated that the recombination reaction didn't increase with the growth of ZnO nanorods on the nanosheets.
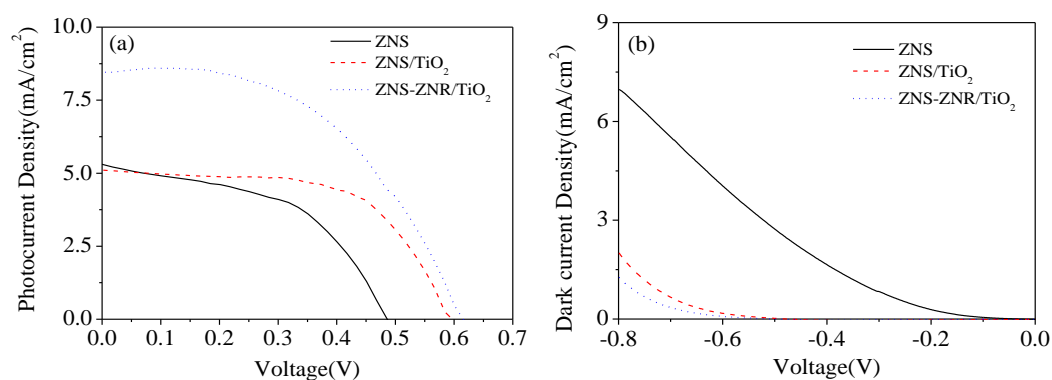
Figure 4. Photocurrent-voltage and dark current-voltage curves of QDSCs based on different photoanodes, ZNS, ZNS/TiO_2 and ZNS-ZNR/TiO_2

Table 1. Photovoltaic Characteristics of QDSCs based on different photoanodes, ZNS, ZNS/TiO$_2$ and ZNS-ZNR/TiO$_2$

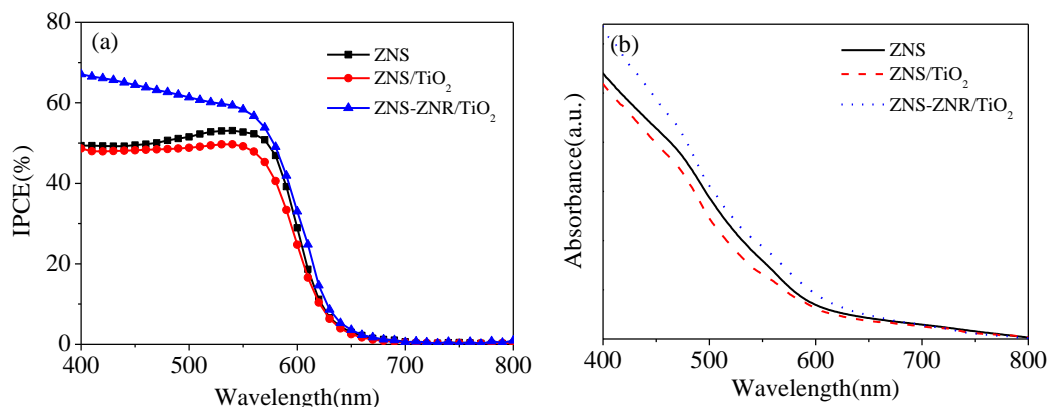| Photoanodes	V_{oc}/V	J_{sc} mA/cm^2	fill factor	Efficiency/%
ZNS	0.485	5.30	0.51	1.31
ZNS/TiO$_2$	0.599	5.19	0.61	1.85
ZNS-ZNR/TiO$_2$	0.616	8.51	0.48	2.50

Figure 5. IPCE spectrum of QDSCs based on different photoanodes, ZNS, ZNS/TiO$_2$ and ZNS-ZNR/TiO$_2$

Figure 5 shows the IPCE (a) and visible absorption spectra of the different photoanodes as a function of wavelength ranging from 400 nm to 800 nm. The absorption extended to 650 nm which was the band edge of CdSe QDs. The absorption edge was almost the same for these three photoanodes which indicated the preparation process were exactly reproduced in the sensitization process. It is well known that the IPCE is directly related with the J_{sc} of QDSCs. It can be seen that the changing trend of IPCE based on different photoanodes was consistent with that of short circuit current in Figure 4 and Tab. 1. The ZNS-ZNR/TiO$_2$ photoanode had the highest IPCE value which affirmed the results of photocurrent-voltage experiments, especial at the wavelength ranging from 400 to 500 nm. The visible absorption spectra of the different photoanodes were also measured to explore the reason for this phenomenon. It can be seen that the absorption value of ZNS-ZNR/TiO$_2$ photoanode was obviously higher than that of ZNS and ZNS/TiO$_2$ photoanodes during the wavelength from 400 to 500 nm which is in accordance with the absorption of CdS QDs. L.B. Li et al. found that the existence of ZnO nanorods on nanosheets could enormously enlarge the light-scattering ability of ZnO films, which might be another reason for the increasing of IPCE value for ZNS-ZNR/TiO$_2$ photoanode [25]. This result indicated that the growth of ZnO nanorods might be favorable for the deposition of CdS QDs during the sensitization processes.

4. CONCLUSION

ZnO nanosheets were electrodeposited on transparent conductive glass substrates. Thereafter, ZnO nanorods were grown vertically on the nanosheets by hydrothermal method to prepare the

nanosheets-nanorods hierarchically structured ZnO films. The concentration of $Zn(NO_3)_2 \cdot 6H_2O$ and $C_6H_{12}N_4$ showed great influence on the preparation process of ZnO nanorods on nanosheets. Regular nanorods could be grown on the nanosheets when the concentration is 0.05 M. The length of ZnO nanorods could grow to be ca. 1.5 μm. The obtained nanosheets-nanorods hierarchically structured ZnO films were co-sensitized with CdS and CdSe quantum dots and applied as the photoanodes of dye-sensitized solar cells. The recombination reaction of this photoanode could be efficiently suppressed with the surface coating of TiO_2. The growth of ZnO nanorods might be favorable for the deposition of CdS QDs and improve the IPCE value at the wavelength from 400 to 500 nm. A photoelectric conversion efficiency of 2.50% was obtained after the coating of TiO_2 on the ZnO nanosheets-nanorods.

CONFLICTS OF INTEREST
The authors declare that there is no conflict of interest regarding the publication of this article.

References

1. A. Yella, H.W. Lee, H.N. Tsao, C.Y. Yi, A.K. Chandiran, M.K. Nazeeruddin, E.W.G.Diau, C.Y. Yeh, S.M. Zakeeruddin and M. Grätzel, *Science,* 334 (2011) 629.
2. W. T. Sun, Y. Yu, H. Y. Pan, X. F. Gao, Q. Chen and L. M. Peng, *J. Am. Chem. Soc.*, 130 (2009) 1124.
3. D. R. Baker and P.V. Kamat, *Adv. Funct. Mater.*, 19 (2009) 805.
4. X.Y. Chen, T. Ling and X.W. Du, *Nanoscale*, 4 (2012) 5602.
5. H. Lee, M. K. Wang, P. Chen, D. R.Gamelin, S.M. Zakeeruddin, M. Grätzel and M. K. Nazeeruddin, *Nano Lett.*, 9 (2009) 4221.
6. J. H. Bang and P. V. Kamat, *ACS Nano*, 3 (2009) 1467.
7. B. R. H.yun, Y. W. Zhong, A. C.Bartnik, L. F. Sun, H. D. Abruna, F. W. Wise, J. D. Goodreau, J. R. Matthews, T. M. Leslie and N. F. Borrelli, *ACS Nano*, 2 (2008) 2206.
8. S. A. McDonald, G. Konstantatos, S. G. Zhang, P. W. Cyr, E. J. D. Klem, L. Levina and E. H. Sargent, *Nature Mater.*, 4 (2005) 138.
9. Y. Y. Xi, Y. F. Hsu, A. B. Djurišić, and W. K. Chan, *J. Electrochem. Soc.*, 155 (2008) 595.
10. K.Wessels,M.Wark, and T. Oekermann, *Electrochim. Acta*, 55 (2010) 6352.
11. P. Tiwana, P. Docampo, M. B. Johnston, H. J. Snaith, and L.M. Herz, *ACS Nano*, 5 (2011) 5158.
12. J. J. Tian, Q. F. Zhang, E. Uchaker, R. Gao, X. H.Qu, S. E. Zhang and G. Z. Cao, *Energ. Environ. Sci.*, 6 (2013) 3542.
13. R. Kumar, A. Umar, G. Kumar, H.S. Nalwa, A. Kumar and M.S. Akhtar, *J. Mater. Sci.*, 52 (2017) 4795.
14. R. Vittal and Kuo-Chuan Ho, *Renewable Sustaninable Energ. Rev.*, 70 (2017) 920.
15. D.P. Wu, X.L. Wang, K. Cao, Y.P. An X.H. Song, N. Liu, F. Xu, Z.Y. Gao and K. Jiang, *Electrochim. Acta*, 231 (2017) 1.
16. S.B. Patil and A.K. Singh, *Electrochem. Acta*, 56 (2011) 5693.

17. Y.Y. Bu, Z.Y. Chen, W.B. Li and J.Q. Yu, *ACS Appl. Mater. Interface*, 5 (2013) 5097.
18. X. P. Qi, G. W. She, Y. Y. Liu, L. X. Mu and W. S. Shi, *Chem. Commun*., 48 (2012) 242.
19. H.N. Chen, W.P. Li, H.C. Liu and L.Q. Zhu, *Electrochem. Commun*., 13 (2011) 331.
20. S.J. Li, Z. Chen, T. Li, H.P. Gao, C.C.Wei, W. Li, W.P. Kong and W.F. Zhang, *Electrochim. Acta*, 127 (2014) 362.
21. J. Tian, E. Uchaker, Q. Zhang and G. Cao, *ACS ACS Appl. Mater. Interface*, 6 (2014) 4466.
22. F. Xu, M. Dai, Y. Lu andL. Sun, *J. Phys. Chem*. C, 114 (2010) 2776.
23. H.L. Feng, W.Q. Wu, H.S. Rao, L.B. Li, D.B.Kuang and C.Y.Su, *J. Mater. Chem*. A, 3 (2015) 14826.
24. A. Roy, P.P. Das, M. Tathavadekar, S. Das and P. S. Devi, *Beilstein J. Nanotech*., 8 (2017) 210.
25. L.B. Li, W.Q. Wu, H.S. Rao, H.Y. Chen, H.L. Feng, D.B. Kuang, C.Y. Su, *Sci. China Mater*., 59 (2016) 807.